Kodaikanal Obs. Bull. (1997) 13, 133-141

Lunar Occultation Observations of the Microwave Sun During the Eclipse of October 24, 1995

J. Bagchi, K.R. Subramanian, E. Ebenezer, N. Gowda, and A.T. Abdul Hameed
Indian Institute of Astrophysics, Bangalore 560 034, India

Abstract

The interpretation of the lunar occultation data recorded at the microwave frequencies of 2.25, 3.80 and 4.20 GHz from two stations during the October 24, 1995 solar eclipse in India is presented.

Key Words : Solar eclipse, Lunar occultation, Microwave emission, Active regions, X-ray emission.

Introduction

At radio wavelengths high angular resolution (≈1") information on solar active regions can only be obtained using multi-element interferometric arrays. A solar eclipse event could be used to advantage to obtain high resolution information even with a moderate sized radio dish due to wave diffraction effects on the lunar limb. In the past many years this method has yielded valuable data on solar limb brightening (Christiansen and Warburton 1950, Hagen 1956, Krishnan and Labrum 1961), identification of the radio emitting active spots and plages (Covington 1947, Kundu 1959, Gary and Hurford 1987) and recognition of sources of suprathermal microwave emission (Correia, Kaufmann and Strauss 1992). The Lunar Occultation method can give an angular resolution of $\theta_F \approx 1''$ at centrimetric radio wavelengths, θ_F being the angular width of the first Fresnel zone. In practice, the limitation is set by the ability of the radiometer to detect small flux changes over the strong quiet-sun background within the short integration time and by the ambiguity of identifying the active regions across the lunar limb. It requires a radiometer of high internal stability with a short sampling period and simultaneous measurements from two or more stations situated at widely spaced locations along the path of lunar shadow to meet the full objectives of an occultation experiment.

Radiometric data recorded at two stations in India during the last October 24, 1995 eclipse and its interpretation forms the subject of this paper.

Observation Procedure and Instrumental Set Up

The circumstances of the eclipse calculated for the observing stations Nim Ka Thana (NKT) and Shriharikota (SHAR) in India are given in the Table 1.

Table 1. Circumstances of the October 24, 1995 eclipse

Station Location	I Contact	IV Contact	Maximum Phase	Fractional Solar Area Occulted At Maximum
Nim Ka Thana	01:54:14	04:19:56	03:02:43	1.00
27° 44' 16.08" N	UT	UT	UT	
75° 47' 46.32" E				
400.0 mts.				
Shriharikota	02:03:11.25	04:30:52	03:12:12	0.56
13° 40' 25.86" N	UT	UT	UT	
80° 11' 46.11" E				
– 72.5 mts.				

The GPS (Global Positioning System) receivers positioned at both the stations provided positional data to within ± 100 m and time information to an accuracy of ± 0.1s.

A parabolic radio dish of 10m diameter tracked the sun at SHAR station (operated by Indian Space Research Organization), recording the radio intensity fluctuations in total power mode in R and L circular polarizations. The centre frequency of observations was 2.25 GHz and the sampling interval 0.3 s.

At NKT station we used a parabolic dish antenna of 2.1 m diameter. Single linear polarization data were recorded in total power mode. The dual centre frequencies were 3.8 GHz and 4.2 GHz and the sampling time was 0.1 s. A series of drift scans, each of about 10 minutes duration, were taken over the sun due to unsatisfactory operation of the track facility. This did not allow us to calibrate the flux density in absolute sense and only relative intensities (for a given scan) could be obtained.

The flux calibration from SHAR station was obtained by assuming an uneclipsed solar flux value of 67.0 ± 0.5 s.f.u. (1s.f.u. = 10^{-22} Wm^{-2} Hz^{-1}) at 2.25 GHz obtained by interpolating between flux values measured at different frequencies on the day of eclipse (Solar - Geophysical Data).

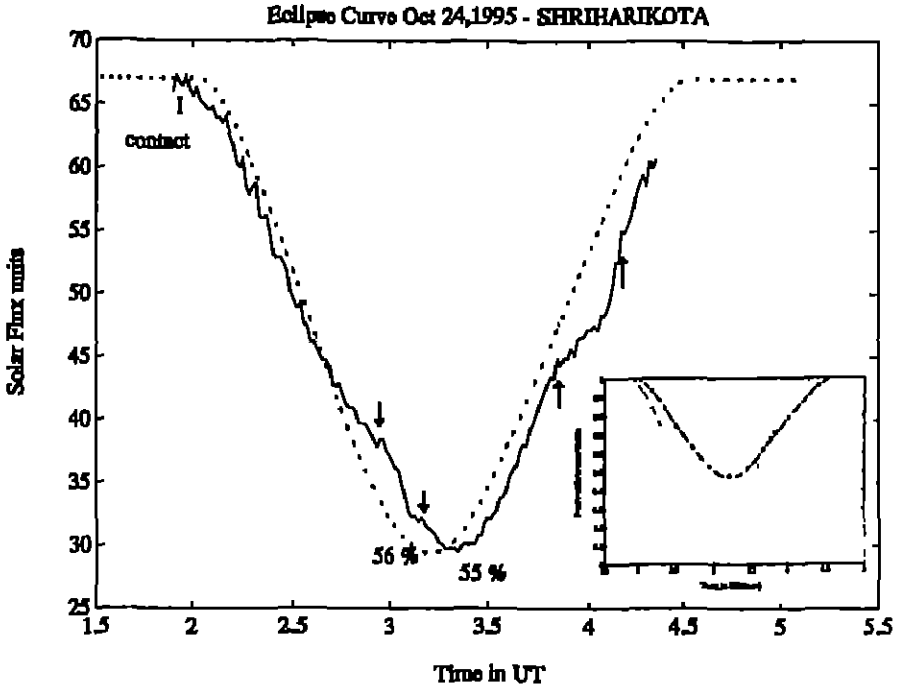

Figure 1a : Theoretical and the observed eclipse curves. The eclipse curves for SHAR station showing the theoretical (dotted) and the observed 2.25 GHz (full line) flux curves. The arrowed sections represent the ingress and egress events. Inset shows the theoretical curves for NKT (dotted) and the SHAR (dash-dotted) stations.

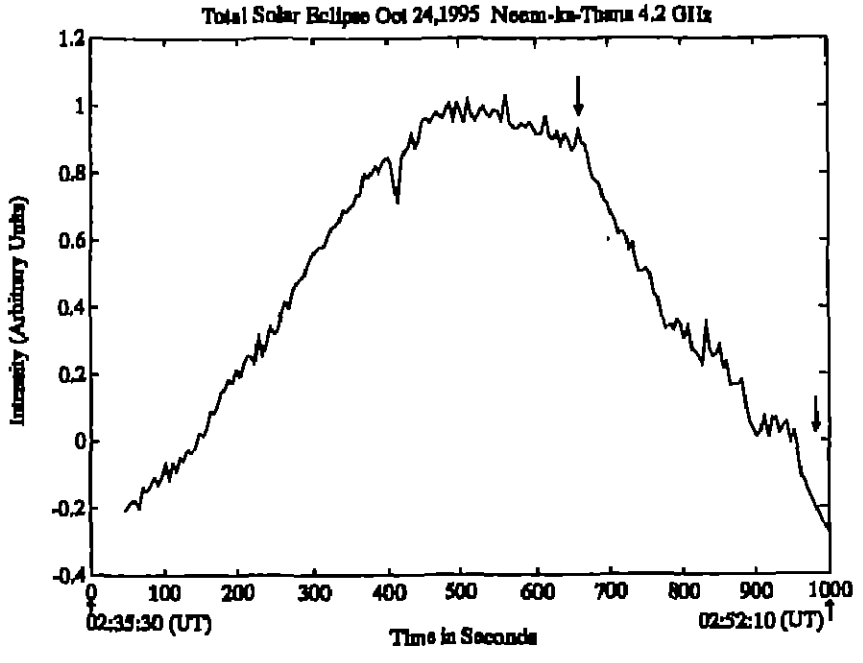

Figure 1b : The drift scan at 4.2 GHz recorded at NKT station (not corrected for the drift profile) near 02:46 UT. The arrowed section between 02:46 UT and 02:52 shows the ingress of an active region. The data at 3.8 GHz (not shwon) is very similar.

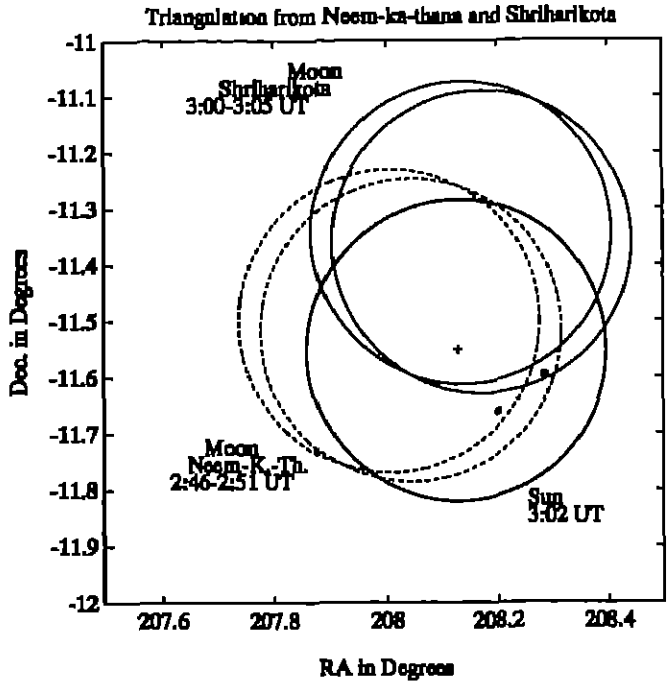

Figure 2a : Identification of the active regions on the solar disk drawn at 03:02 UT (heavy circles). The positions of the lunar limb at 03:00 and 03:05 UT from SHAR station (light circles) and at 02:46 and 02:51 UT from NKT station (dotted circles) are shown. The positions of two identified active regions are shown by black dots. The '+' symbol is at the Sun centre.

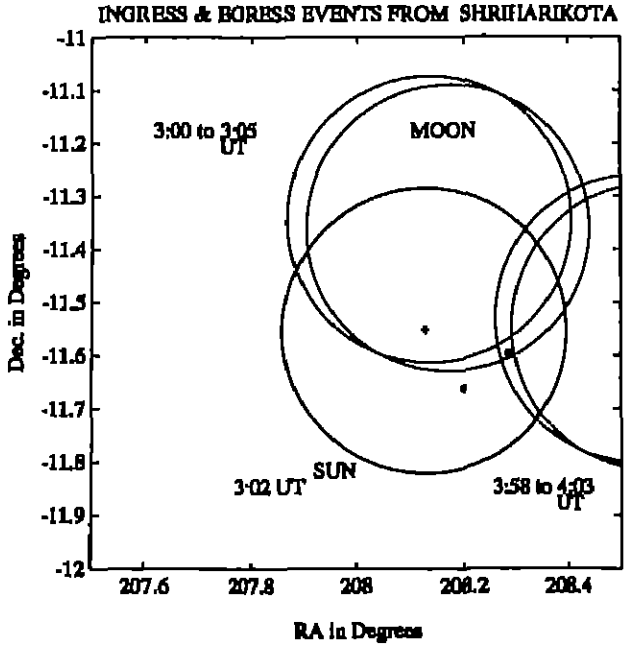

Figure 2b : The lunar limb positions computed for SHAR station at ingress (03:00 to 03:05 UT) and egress (03:58 to 04:03 UT) of an active region. Two black dots denote the two identified active regions. The '+' symbol is at the centre of the Sun. Note that the North is up and East is to the right on these figures.

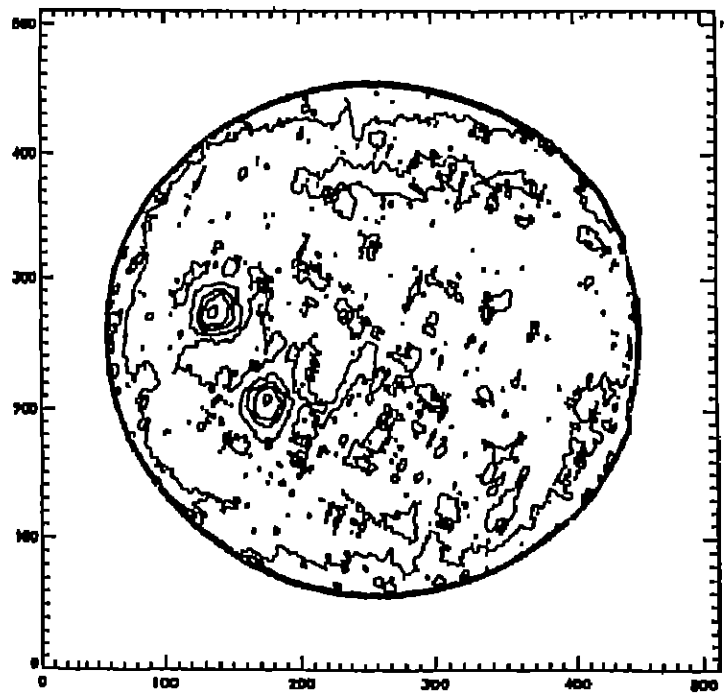

Figure 3a : The Nobeyama 17 GHz solar image at 03:02 UT. The image resolution is about 15 arcsec and the total intensity (unpolarized) data is shown. The peak brightness temperature for both the sources on the east is $\approx 1.5 \times 10^4$ K. The quiet-sun disk temperature is $\approx 10^4$ K. Solar north is at top and east to the left.

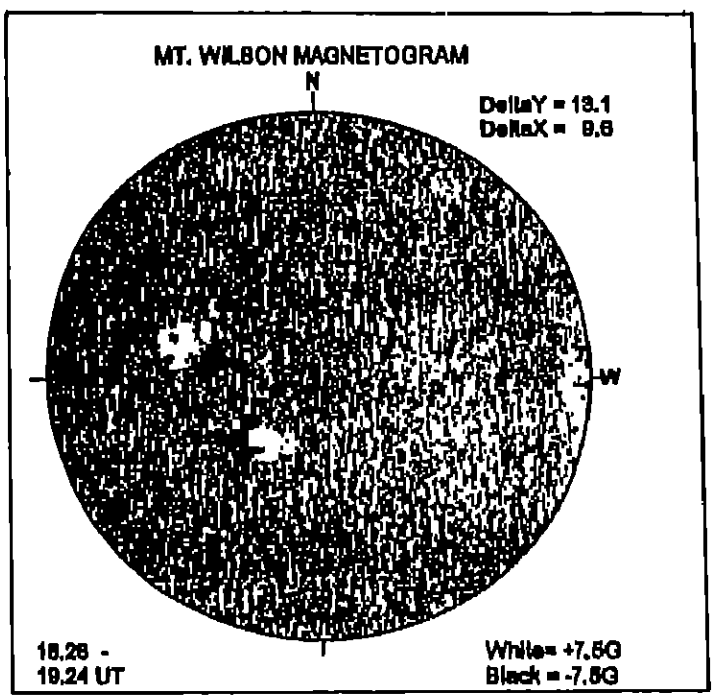

Figure 3b : The magnetogram taken at Mt. Wilson Observatory at near 19.00 UT. Bright represents positive and dark the negative magnetic polarity.

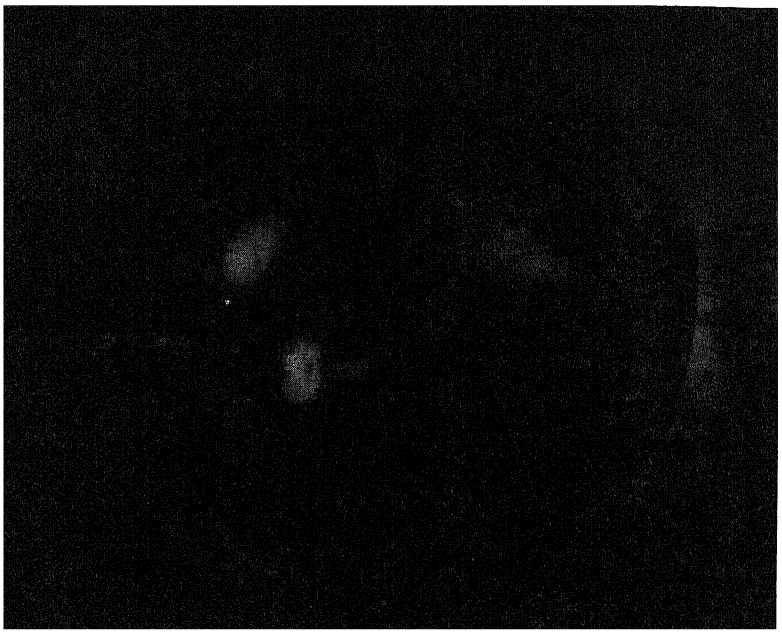

Figure 3c : Soft X-ray (4 to 60Å) image of the Sun taken at 08:49 UT by the telescope at YOHKOH satellite. The image has the resolution of about 3 arcsec. The solar north is at top and east to the left.

Analysis and Observational Results

Theoretical eclipse curves for both stations were computed using data on Lunar Besselian Polynominal Coefficients and a uniformly bright solar disk model. These curves are given in Fig. 1. The data from SHAR station were averaged for 1 minute intervals and the light-curve overlayed on the theoretical curve to look for sudden intensity and slope variations (Fig. 1a). Such variations possibly signify the ingress or egress of radio emitting components behind the lunar limb. No significant difference in the intensity for R and L polarizations could be detected. We therefore discuss only the total intensity (R+L) data here.

Examination of eclipse data from SHAR station reveals a sudden flux decrement during ingress phase between 02:57:46 UT and 03:06:46 UT and another abrupt flux increment during egress lasting from 03:56:00 UT to 04:05:00 UT (arrowed times on Fig. 1a). The slope of the observed curve departed significantly from the theoretical slope at these times. The observed flux-density changes due to both these events were 9.0 ± 1.0 s.f.u. From slope measurements on the theoretical curve, the flux contribution of 6.0 s.f.u. could be attributed to the quiet-sun radio emission. The residual 3.0 s.f.u. is thus possibly due to the presence of some active region on the Sun.

Both the 4.2 GHz and the 3.8 GHz drift scans taken from NKT station near 02:46 UT also revealed a sudden flux decrement between the times 02:46:00 UT and 02:52:00 UT during the ingress phase of the eclipse (arrowed, Fig. 1b). The intensity is shown in arbitrary units, normalised to unity at peak intensity for the scan. The egress phase of this event could not be recorded as it fell between two successive scans.

Identification of the Active Region

Due to one dimentional nature of the scan by the entire lunar limb, locating the radio emitting region on the sun is not possible from data taken from a single station alone. Therefore, we have performed a 2-station triangulation analysis. The lunar limb positions, as observed from SHAR and NKT stations, corresponding to the times of sudden flux decrements (ingress) were computed and plotted on the solar disk (Fig. 2a). The trajectory of the moon is approximately solar NW to SE across the solar disk. A pair of diamond shaped areas, bounded by lunar limbs, then gives the likely location of the radio source. Only one solution falls on the solar disk. The other, although mathematically valid, is located far outside the west limb and therefore is unphysical. To check for the validity of the disk bound solution, we have plotted the lunar limb positions at both the ingress and the egress events observed from SHAR station alone. This solution, shown in Fig. 2b, again locates the active region almost exactly on the earlier disk bound solution. The second solution is once more located far outside the solar disk and not coincident with the earlier solution. Thus, the unique and physically unambiguous location for the radio source is within the diamond shaped region ≈ 10' to the south-east of the sun centre at a position angle of 105 degrees east from north (Fig. 2, a and b). The estimated uncertainty in this position is about ± 0.5 minute of arc.

Discussion and Conclusions

From the slope of the occultation curve at 2.25 GHz from SHAR and assuming an angular speed of 0.55 arcsec s^{-1} of moon relative to sun during eclipse, we have obtained the full width deconvolved angular size of 5.0 ± 1.0 arcminutes for the identified active region. The implied brightness temperature T_b at 2.25 GHz is thus 1.2×10^5 K. Due to smoothening of the data over 1 minute intervals, features with angular sizes < 1' were not recognized and the presence of one or more compact regions with significantly higher brightness temperatures can not be ruled out in this active region.

Towards understanding the nature of this radio source, we have searched and compared our data with available solar data at other wavelengths on the day of the eclipse. These are discussed below.

Nobeyama 17 GHz Solar Image

The 17 GHz solar image from Nobeyama Radio Observatory (Nakajima, 1994), at a resolution of ≈ 15", taken at around 03:02 UT, is shown in Fig. 3a. Two radio emitting spots on the eastern half of the sun are visible on this total intensity (unpolarized) image. The northern source could be unambiguously identified with the active region position obtained from our eclipse data at 2.25 GHz and 4.2 GHz (Fig. 2). The peak brightness temperatures T_b for both the spots are ≈ 1.5×10^4 K implying a fall of T_b by at least a factor of 10 between 2.25 and 17 GHz frequencies. The angular size of 3.0 ± 0.5 arcmin for the northern source is considerably smaller than its size of 5.0 ± 1.0 arcmin at 2.25 GHz. This could either imply the expansion of the radio plasma between the two levels of emission or alternatively, scatter broadening of the

radio waves at the lower frequency. No multiple components within the radio structures could be identified at the available resolution of ≈ 15 arcsec, but elongation of the sources could be seen on the 17 GHz map. The lunar limb just grazed the southern spot (Fig. 2b), resulting in a negligible flux variation near the maximum phase. We could not identify this feature on our eclipse light curves.

YOHKOH soft X-ray image and the Solar Magnetogram

The magnetogram obtained at the Mt. Wilson Observatory near 19:00 UT is shown in Fig. 3b. Two prominent active regions with bipolar magnetic fields and flipped polarities in the northern and the southern hemispheres are apparent. Two sunspot groups No. 7918 (north) and No. 7917 (south) associated with the magnetic features, were present on the day of the eclipse (Solar-Geophysical Data).

The YOHKOH soft X-ray telescope image in 4 to 60 Å wavelength band (Tsuneta *et al.*, 1991) taken near 08:49 UT is shown in Fig. 3c. At an image resolution of ≈ 3" many interesting features could be identified. Noteworthy are the two intense X-ray emitting structures identified with the Nobeyama 17 GHz radio-hot-spots and the bipolar magnetic features seen on the magnetogram. The northern X-ray feature is associated with the radio source identified by us from eclipse records.

The morphology of X-ray emission from these structures is clearly that of arch-shaped flux-tubes containing the hot plasma. Intense X-ray brightening over the central sections of both the arches could be seen. On comparing the magnetogram with the X-ray image we infer that the foot-points of these arches are probably rooted in the magnetic poles of opposite polarities and the topmost section of each, containing individual local X-ray hot spots, crosses the zone between the opposite magnetic polarities almost parallel to the neutral line. Such an arch-configuration has been noted earlier in lower resolution X-ray images from the SKYLAB mission (Schmahl 1980).

Due to limitations imposed by lower resolution available on the 17 GHz radio map, full details of the radio morphology are not visible, but it is apparent that the peak radio emission comes close to the regions of maximum X-ray brightness. Earlier high resolution radio data at 11.7 GHz on many active regions have shown that they may possess bright cores and are usually associated with either a plage or a polarity reversal, tending to be brighter near the locations of larger shear in the magnetic field (Gaizauskas and Tapping 1988). Comparison of the 17 GHz radio image and the X-ray image of two active regions indicates that the major axes of the X-ray emission lie along the same directions as the major axes of the radio features and their angular sizes are also comparable. These data indicate that the component plasmas radiating the radio and the soft X-rays are probably closely associated and the morphology of the radiating gas is probably governed by the structure of the magnetic field lines over the active regions.

It is not immediately clear what is the principal emission process at 17 GHz. The association observed above could imply a large contribution due to thermal-bremsstrahlung process. However, at 17 GHz, some active regions with kilo-Gauss fields, emitting mainly due to magneto-gyroresonance process have been noticed recently (Shibasaki *et al.*, 1994). High degree of circular polarization with radiation originating over a region of intense magnetic field are the signatures of this process. Detailed, polarization data are required to study this aspect further.

Thus to conclude, the lunar occultation observations have provided useful data on solar activity on the day of eclipse. The high resolution information provided by the occultation technique, when combined with the data from two points along the lunar shadow, have enabled us to locate the position of the active radio region on the solar disk unambiguously. We conclude that the brightness temperature of this source is about a factor of 10 higher at 2.25 GHz, compared to its value at 17 GHz. The angular size was found to be substantially larger at 2.25 GHz. Intense, arch-shaped X-ray emitting structures over the bipolar magnetic zones could be identified on the X-ray image. The close similarity of angular sizes, position angles and the location of brightest regions for these structures from 17 GHz to X-ray frequencies possibly imply a close association of the emitting plasma, its radiative properties and the morphology shaped by the local magnetic field configuration.

Acknowledgements

We thank Prof. R. Cowsik and Prof. Ch. V. Sastry of IIA for their kind help and support for this work. We express our gratitudes to Drs. A. Deshpande and S. Chandrasekhar of RRI, Bangalore for their interest and valuable timely help. The researchers of ISTRAC centre, Bangalore are thanked for sharing their data with us. Prof. Jagdev Singh and Prof. P. Venkatakrishnan of IIA provided us with all the possible help during the eclipse expedition. We also thank all the staff memebrs of IIA for their cooperation at the eclipse camp.

References

Christiansen W.N., Warburton, J.A. 1950, Aust. J. Phys., **A6**, 190.
Correia E., Kaufmann, P., Strauss, F.M. 1992, Sol. Phys., **138**, 223.
Covington A. 1947, Nature, **159**, 405.
Gaizauskas V., Tapping, K.F. 1988, Astrophys. J., **325**, 912.
Gary D.E., Hurford, G.J. 1987, Astrophys. J., **317**, 522.
Hagen J.P. 1956, Solar Eclipses and the Ionosphere, (Pergamon Press, London), p. 253.
Krishnan T., Labrum, N.R. 1961, Aust. J. Phys., **14**, 403.
Kundu M.R. 1959, Ann. Astrophys., **22**, 1.
Nakajima H., *et al.* 1994, Proc. IEEE, **82**, No. 5, 705.
Schmahl E. 1980, Radio Physics of the Sun, (IAU Symp. 86, Kundu, M.R., and Gergely, T.E., eds.).
Shibasaki K., *et al.* 1994, Publ. Astr. Soc. Japan, **46**, L17.
Tsuneta S., *et al.* 1991, Sol. Phys., **136**, 37.